Albumin Binding to FcRn: Distinct from the FcRn−IgG Interaction†

Chaity Chaudhury,‡ Charles L. Brooks,§ Daniel C. Carter,|| John M. Robinson,⊥ and Clark L. Anderson*,‡

Departments of Internal Medicine, Veterinary Biosciences, and Physiology and Cell Biology, The Ohio State University, Columbus, Ohio 43210, and New Century Pharmaceuticals Inc., Huntsville, Alabama 35824

Received December 23, 2005; Revised Manuscript Received February 2, 2006

ABSTRACT: The MHC-related Fc receptor for IgG (FcRn) protects albumin and IgG from degradation by binding both proteins with high affinity at low pH in the acid endosome and diverting both from a lysosomal pathway, returning them to the extracellular compartment. Immunoblotting and surface plasmon resonance studies show that both IgG and albumin bind noncooperatively to distinct sites on FcRn, that the affinity of FcRn for albumin decreases ≈200-fold from acidic to neutral pH, and that the FcRn−albumin interaction shows rapid association and dissociation kinetics. Isothermal titration calorimetry shows that albumin binds FcRn with a 1:1 stoichiometry and the interaction has hydrophobic features as evidenced by a large positive change in entropy upon binding. Our results suggest that the FcRn−albumin interaction has unique features distinct from FcRn−IgG binding despite the overall similarity in the pH-dependent binding mechanism by which both ligands are protected from degradation.

The MHC-related receptor for IgG (FcRn),[1] binding IgG in a pH-dependent fashion, functions both to transport IgG peripartum from mother to young and to protect it from degradation throughout life (*1*). The proposed mechanism for transport, a pH-dependent shuttle, is essentially identical to that for protection. IgG is pinocytosed nonspecifically by the cell and is trafficked to the acidic endosome where in the low pH environment it binds FcRn with high affinity. FcRn then diverts (or protects) IgG from a degradative lysosomal fate, instead transporting it back to the cell surface for release into the extracellular space. At the cell surface under the influence of neutral pH the affinity of IgG for FcRn is reduced by over 2 orders of magnitude, and the half-life ($t_{1/2}$) of the FcRn−IgG complex decreases 10−30-fold, allowing the complex to dissociate (*2*−*7*). The lengthy 3 week half-life of IgG and its unusual concentration−catabolism relationship are thus explained (*8*−*11*). Remarkably, albumin uniquely shares with IgG two FcRn-dependent properties, viz., its lengthy 3 week half-life and the same unusual direct concentration−catabolism relationship, suggesting that albumin as well may be protected from degradation by the same mechanism proposed for IgG (*12*).

In our recent work we discovered that FcRn binds albumin in a pH-dependent fashion. Exploring the functional importance of FcRn−albumin binding in FcRn-deficient mouse strains, we found that the half-life and the steady-state concentration of albumin were decreased in the KO strains relative to the wild-type strain (*13*). The magnitude of albumin saved from degradation by FcRn-mediated recycling is astonishing. Our recent calculations indicate that as much albumin is saved by FcRn from degradation as is produced by the liver per unit time; metaphorically, a mouse lacking FcRn would require another liver the size of its existing liver to maintain albumin concentrations at steady state (*14*). Unifying these several observations, we propose that FcRn diverts not only IgG but albumin as well from a degradative fate by similar pH-dependent mechanisms, prolonging the life spans of both molecules and accounting for their uniquely direct concentration−catabolism relationship.

The impact of FcRn on basic physiology is profound, as its two ligands, albumin and IgG, constitute about 80% of the protein mass of plasma. Both molecules mediate essential life functions. One, IgG, is a critical component of the immune system. The other, albumin, maintains the colloid osmotic pressure of the circulation, buffers the pH of plasma, and transports a myriad of molecules including biological products, toxins, drugs, and therapeutic proteins throughout the body.

While FcRn's role in IgG transport and protection has been well characterized, virtually nothing is known about the FcRn−albumin interaction and the mechanism of FcRn-mediated albumin transport and protection beyond our initial report (*13*). We present here the first description of the biochemical details of this newly discovered receptor−ligand interaction and report that the overall mechanism of albumin binding by FcRn, while similar to that for IgG, has unique characteristics.

MATERIALS AND METHODS

Proteins. The Chinese hamster ovary (CHO) cell line 2G11 secreting recombinant soluble human Fc receptor (shFcRn),

† This work was supported in part by Grants HD38764, CA88053, and AI057530 from the NIH.

* Corresponding author. Phone: (614) 247-7650. Fax: (614) 247-7669. E-mail: anderson.48@osu.edu.

‡ Department of Internal Medicine, The Ohio State University.

§ Department of Veterinary Biosciences, The Ohio State University.

|| New Century Pharmaceuticals Inc.

⊥ Department of Physiology and Cell Biology, The Ohio State University.

[1] Abbreviations: shFcRn, soluble human Fc receptor (neonatal); HSA, human serum albumin; hIgG, human immunoglobulin G; CHO, Chinese hamster ovary; SPR, surface plasmon resonance; ITC, isothermal titration calorimetry; R_{eq}, response at equilibrium; RU, resonance units.

10.1021/bi052628y CCC: $33.50
Published on Web 03/22/2006

given by Dr. Pamela Bjorkman (California Institute of Technology, Pasadena, CA), was cultured in custom α MEM Earle's medium (Irvine Scientific) with 5% fetal calf serum, penicillin, streptomycin (Invitrogen), and methyl sulfoximine (Sigma-Aldrich) essentially as described (*15*). shFcRn was purified from the culture supernatant by affinity chromatography followed by anion-exchange chromatography, as described, that yielded two separate peaks, shFcRn and BSA, each uncontaminated by the other according to SDS−PAGE and Coomassie staining (*13*, *15*). The hIgG2 myeloma protein (catalog no. 40012) was purchased from Calbiochem, nondelipidated human serum albumin (HSA; catalog no. A-8763) and hIgG (catalog no. I-4506) were from Sigma-Aldrich, and the four delipidated recombinant HSA domains, domains I (D-I), II (D-II), III (D-III), and I-II (D-I-II) encompassing amino acids 1−197, 189−385, 381−585, and 1−385, respectively, were kindly provided by Dr. Dan Carter (*16*).

Dynamic Light Scattering (DLS) Analysis. The homogeneity of the HSA was confirmed by DLS analysis of 10 or 100 μM HSA solutions in 50 mM sodium phosphate and 150 mM NaCl, pH 5.5, buffer using the DynaPro instrument and software (Protein Solutions). The data fit a monomodal model with a mean molecular mass of 72.7 ± 2.4 kDa, suggesting a monodispersed preparation with no measurable aggregates (less than 2−3%).

Size Exclusion Chromatography. HSA was resolved on a 2.5 × 80 cm Sephacryl S-300 (catalog no. 17-0599-01) size exclusion column (Amersham Biosciences) in 50 mM sodium phosphate and 150 mM NaCl, pH 5.5, buffer at 1 mL/min; the eluting peak fractions were visualized by monitoring UV absorption at 280 nm (A_{280}) and collected.

SPR Measurements. The equilibrium, association, and dissociation rate constants were measured at 25 °C on a Biacore 3000 surface plasmon resonance biosensor and the data analyzed using the BIAevaluation 3.1 software (Biacore International AB). HSA or shFcRn was covalently immobilized at three different densities (∼500, 1000, and 1500 RU) on a CM5 chip (catalog no. BR-1000-14) using amine coupling (Biacore Handbook, 2002). One of the flow cells was mock coupled with 50 mM sodium phosphate and 150 mM NaCl buffer of appropriate pH to serve as blank. All of the injections were made in 50 mM phosphate and 150 mM NaCl buffer of appropriate pH (between 5 and 7), and the chip surface was regenerated between injections with pH 8.1, 20 mM Tris buffer. The purity of both HSA and shFcRn used in these experiments was ∼99% as visualized on a 10% SDS−polyacrylamide sizing gel under reducing conditions by Coomassie blue staining. The protein concentrations were determined by the bicinchoninic acid (BCA) protein assay kit (catalog no. 23227; Pierce Chemical Co.) using BSA as standard. The concentration of the standard was determined by A_{280}.

To measure equilibrium dissociation constants (K_D), increasing concentrations of the analyte, shFcRn (10 nM−35 μM) or HSA (10 nM−250 μM), were injected at 5 μL/min over immobilized ligand (HSA or shFcRn). The binding was allowed to reach equilibrium, and the K_D was derived by fitting the plot of the binding response at equilibrium (R_{eq}) vs analyte concentration to a steady-state affinity model using nonlinear regression analysis.

On-rate (k_a) and off-rate (k_d) constants were calculated by injecting increasing concentrations of analyte, shFcRn (40 nM−10 μM for pH range 5−6 and 40 nM−30 μM for pH 6.5 and 7.0) or HSA (100 nM−100 μM for pH range 5.0−6.0 and 100 nM−250 μM for pH 6.5 and 7.0) at a flow rate of 50 μL/min, for 120 s followed by a 120 s dissociation phase over the immobilized ligand. The sensorgrams were fit to a 1:1 Langmuir binding model which simultaneously fits the association and the dissociation phases of the sensorgrams and globally fits all curves in the working set to derive k_a and k_d. To ensure that mass transport effects do not influence the kinetic measurements and that accurate kinetic information is obtained, the optimal flow rate was first determined in a separate experiment (data not shown). The entire range of analyte concentrations was injected over the immobilized ligand at different flow rates (25, 50, 75, and 100 μL/min), and the slope (RU/s) of the initial 10% of the association phase vs flow rate was plotted for each analyte concentration. The flow rate at or above which the slope did not change with increasing flow rate was chosen as appropriate.

Isothermal Titration Calorimetry (ITC). A Microcal VP-ITC instrument was used to measure stoichiometry of shFcRn and HSA; the data were analyzed using Origin version 7.0 (OriginLab Corp.). Both HSA and shFcRn were exhaustively dialyzed against 50 mM sodium phosphate and 150 mM NaCl, pH 6.0, buffer, filtered, and thoroughly degassed. shFcRn was placed in the calorimetric cell and titrated with HSA in a 300 μL syringe. A total of 19 injections were made. The heat of dilution of HSA was measured in a separate experiment by injecting HSA into the dialysis buffer under identical conditions and subtracted from the shFcRn titration to obtain the heat of binding of HSA to FcRn. The data were fit to a model describing a single class of noninteracting binding sites using nonlinear regression analysis to calculate binding constant (K_A), enthalpy change (ΔH), and stoichiometry (n). The protein concentrations for this experiment were determined by A_{278} and A_{280} for HSA and shFcRn, respectively. The theoretical extinction coefficients of HSA (41012.7 M^{-1} cm^{-1}) and shFcRn (84920 M^{-1} cm^{-1}) under denaturing conditions (6.0 M guanidium hydrochloride and 0.02 M phosphate, pH 6.5) were first calculated from the primary amino acid composition, and the protein concentrations were determined by measuring the UV absorption at the respective wavelengths (*17*). The extinction coefficients of native HSA (37800 M^{-1} cm^{-1}) and shFcRn (84463.2 M^{-1} cm^{-1}) were then calculated from the A_{278} and A_{280} of the known concentrations of these two proteins under nondenaturing conditions (50 mM sodium phosphate and 150 mM NaCl, pH 6.0).

Immnuoblotting. Tris buffer or HSA (substitution ratio of 10 mg of HSA/mL of Sepharose) was immobilized on CNBr-activated Sepharose 4B (Amersham Biosciences) as described (*15*). HSA-linked Sepharose beads (S-HSA) were diluted with Tris-linked beads (to a concentration of ∼18 μg of linked HSA/20 μL of beads), washed with 50 mM sodium phosphate and 150 mM NaCl buffer, pH 5.5, and then incubated for 2 h at room temperature with a fixed concentration of shFcRn (final concentration 75 μg/mL) and varying concentrations of hIgG (75−1200 μg/mL) in 180 μL of 50 mM sodium phosphate and 150 mM NaCl, pH 5.5, buffer. Unbound protein was washed away, and bound

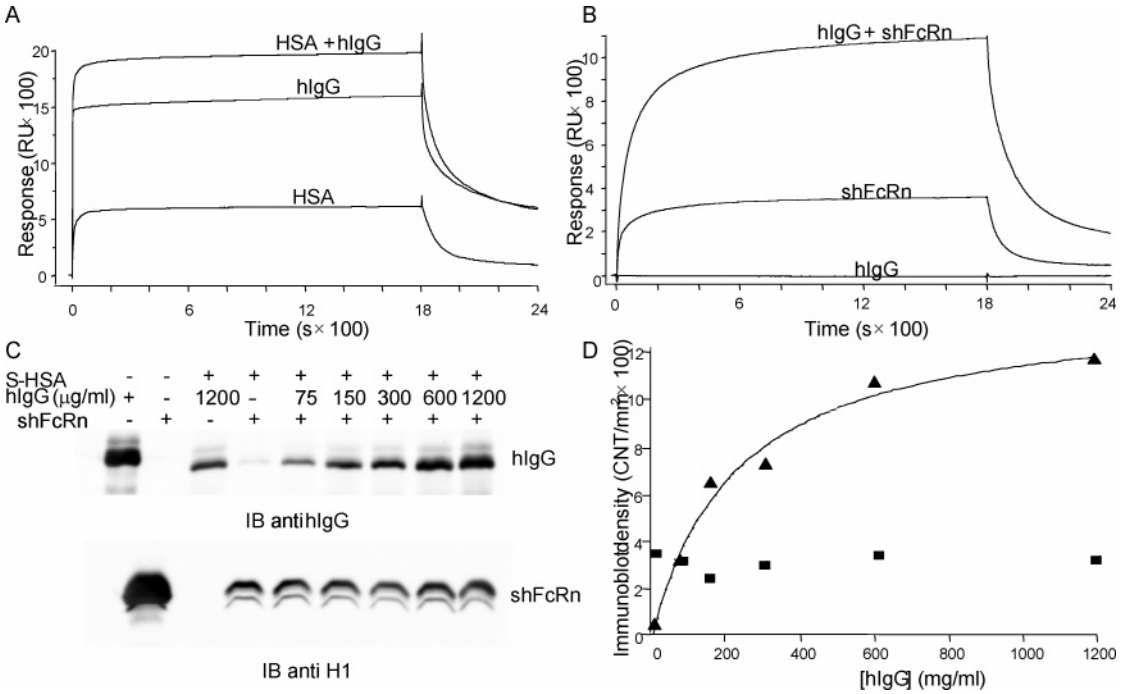

FIGURE 1: SPR and immunoblotting show that hIgG and HSA bind to independent sites on shFcRn and hIgG binding does not affect the HSA−shFcRn interaction. In SPR experiments, 30 μM HSA or 10 μM hIgG or both (as indicated) were injected at 5 μL/min for 1800 s over immobilized shFcRn (845 RU) at pH 5.5. The sensorgrams show the mass (RU) of HSA or IgG or both bound to immobilized shFcRn after blank subtraction on the *Y*-axis vs time in seconds on the *X*-axis (panel A). Panel B shows the sensorgrams of 10 μM hIgG or 2 μM shFcRn or both binding to immobilized HSA (1246 RU) under conditions identical to those in (A). In immunoblotting experiments, samples of Sepharose−HSA were incubated with a fixed concentration of shFcRn and increasing amounts of IgG as shown in panel C. Bound shFcRn and hIgG were eluted and quantified by immunoblotting with anti-hIgG or anti-FcRn antibody. Lanes 1 and 2 in both of the gels contained 4 μg of hIgG and 15 μg of shFcRn. The hIgG (triangle) and shFcRn (square) bands were quantified, nonspecific binding was subtracted, and specific binding was plotted vs hIgG concentration (panel D).

protein was eluted by boiling with SDS-containing sample buffer (60 mM Tris, pH 6.8, 2.3% SDS, 10% glycerol, 0.01% bromophenol blue) containing 1% 2-mercaptoethanol and analyzed on a SDS−polyacrylamide gel followed by immunoblotting with anti-hFcRn (anti-H1) or anti-hIgG-HRP (code no. 709-036-146; Jackson Immunoresearch) antibodies and enhanced chemiluminescence as described (*18*). The amount of shFcRn or hIgG bound to immobilized HSA was quantified with a Fluor-S-Max multiimager using Quantity One software (Bio-Rad). Nonspecific IgG binding, assumed to be linear with respect to IgG concentration (*19*), was subtracted from total binding to give specific binding.

RESULTS

We previously reported that FcRn binds both albumin and IgG in a pH-dependent fashion on independent sites (*13*). Assessing further by SPR whether the two ligands compete for the same binding site or whether they bind to nonoverlapping sites on shFcRn, we found that the amount bound from a mixture of HSA and hIgG injected over immobilized shFcRn equaled the sum of the amounts bound from injections of the individual ligands, HSA and hIgG (Figure 1A). In a second experiment when hIgG, shFcRn, or a mixture of the two was injected over immobilized HSA, the binding response for the mixture was three times the response for shFcRn alone, while hIgG alone did not bind immobilized HSA (Figure 1B). These results indicate that HSA and IgG bind to separate sites on shFcRn.

Assessing if IgG influences the FcRn−HSA interaction, we found that IgG neither enhances nor inhibits the binding of shFcRn to HSA (Figure 1C,D), suggesting that IgG does not cooperatively modulate the FcRn−albumin interaction. When varying concentrations of hIgG and a fixed concentration of shFcRn were incubated with aliquots of Sepharose−HSA (Figure 1C), the amount of hIgG bound to shFcRn increased with increasing hIgG concentration and reached saturation at an IgG:shFcRn molar ratio of 1:1, while the amount of shFcRn bound to HSA remained constant over the entire concentration range of IgG. Moreover, since IgG did not displace shFcRn from HSA, shFcRn must display separate binding sites for both ligands, assuming roughly equivalent affinities.

Isothermal titration calorimetry (ITC) showed that the titration isotherm of FcRn and HSA (Figure 2A, upper panel) is characterized by the absorption of heat. The interaction has a favorable binding free energy ($\Delta G = -7.2$ kcal), despite an unfavorable enthalpy change ($\Delta H = 8.0$ kcal/mol) caused by a large positive entropy change [$\Delta S = 50.1$ cal/(mol·K)] characteristic of hydrophobic interactions. The binding isotherms fit a model characterized by a single class of noninteracting binding sites (Figure 2A, lower panel) and yielded a stoichiometry of 1 and a K_D of 5. 2 μM at pH 6.0 (*20*−*22*). The stoichiometry and thermodynamic parameters obtained in several independent experiments were similar (Figure 2B).

Our previously reported ligand-affinity experiments indicated that shFcRn binds HSA at acidic pH and dissociates at neutral or basic pH (*13*). Extending these observations by surface plasmon resonance (SPR), we measured the K_D of the molecular interaction between soluble human FcRn

A

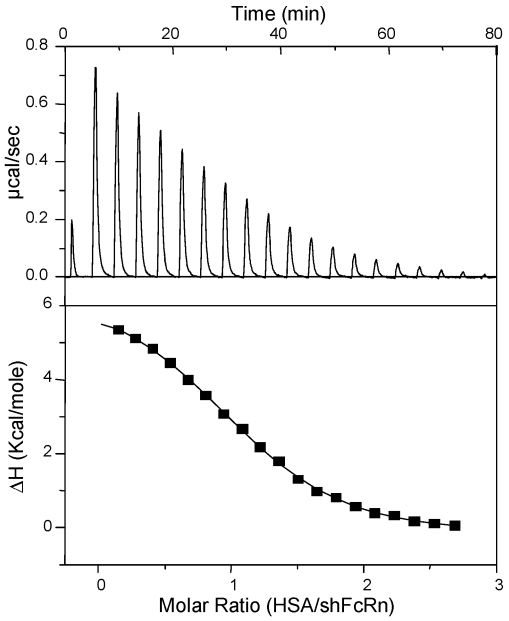

B

Expt	Stoichiometry (N)	K_D (μM)	ΔH (KCal/mol)	ΔS (Cal/mol-K)	ΔG (KCal)
1	1.1	5.6	8.8	53.6	-7.2
2	1.1	4.9	8.3	52.0	-7.2
3	1.0	6.0	9.6	56.2	-7.1
4	1.2	6.9	10.0	57.2	-7.0
5	1.1	6.4	6.8	46.7	-7.1
6	1.0	3.9	6.3	45.8	-7.4
7	1.1	3.1	6.0	45.2	-7.5
Mean ± SD	1.1 ± 0.1	5.2 ± 1.4	8.0 ± 1.6	50.1 ± 5	-7.2 ± 0.1

FIGURE 2: Isothermal titration calorimetry shows an entropically driven interaction and a 1:1 stoichiometry of HSA binding to shFcRn. In the upper panel of (A), HSA (300 μM), as a series of 15 μL injections spaced 280 s apart, was titrated into shFcRn (25 μM), stirred at 300 rpm, and maintained at 25 °C at pH 6.0. In the lower panel of (A), the binding isotherms (symbols) were fit (line) to a model describing a single class of binding sites. The table of panel B shows the thermodynamic parameters obtained by fitting the data to a single class of binding sites in multiple experiments.

(shFcRn) and human serum albumin (HSA) between pH 5 and pH 7. We found that both receptor and ligand bound one another reversibly and the binding response was directly proportional to the concentration of analyte injected when either was immobilized on a dextran-coated surface (CM5 chip). When HSA was injected over immobilized shFcRn, HSA bound reversibly at acidic pH, and the binding attained equilibrium in ~500 s (Figure 3A, inset). The binding response increased linearly with increasing HSA concentration until it reached a plateau at saturating concentrations of HSA. The plot of equilibrium binding response vs HSA concentration fit a model describing a single class of binding sites (Figure 3A) but not a model describing two classes of noninteracting binding sites (two site) or a model describing sequential binding of two sites on the analyte (bivalent analyte) as proposed for IgG and immobilized FcRn (*23*).

Reversing the orientation of receptor and ligand, immobilizing HSA on the chip (Figure 3B, inset), and measuring equilibrium binding of a variety of concentrations of shFcRn, we found that the binding of receptor was also reversible at acidic pH. As with the immobilized receptor, the binding response was proportional to the amount of shFcRn injected, and it plateaued at saturating concentrations. The plot of equilibrium binding response vs shFcRn concentration fits a single class of binding sites model (Figure 3B), but fitting the data to a model describing two classes of noninteracting binding sites or sequential binding of two sites did not improve the quality of fit. Flow cells with ligand densities ranging between 500 and 1500 RU gave similar K_D values (data not shown). We have also immobilized HSA by ligand thiol coupling at Cys 34, the only reduced sulfhydryl group in HSA, measuring binding at pH 6.0 of shFcRn at different concentrations; the K_D (3.53 μM) was similar to those obtained by amine coupling, confirming that amine coupling of HSA does not perturb the shFcRn binding site on albumin (*24*). We also measured the K_D for IgG2 binding to immobilized shFcRn and using a bivalent analyte model found values (2.03 and 3.83 μM for immobilized IgG2; 1 and 311 nM for IgG2 binding to immobilized shFcRn) similar to published results of others (*15*). We note that the K_D is 7-fold higher when the receptor is immobilized than when HSA is immobilized at pH 5.5, but we do not see a change in K_D as dramatic (100-fold) as has been reported for immobilized FcRn (in the nanomolar range) and IgG (in the submicromolar range) (*23*). The higher K_D observed when the receptor is immobilized suggests that free amine containing residues (Arg and Lys) may be present in close proximity to the albumin binding site on FcRn. The presence of a small amount of aggregates in the HSA preparation did not affect the SPR measurements (please see Supporting Information). As expected, the K_D of the shFcRn−HSA interaction increased markedly as the pH changed from acidic (0.2−0.7 μM at pH 5.0) to neutral (34−408 μM at pH 7.0) for both immobilized shFcRn (583-fold) and HSA

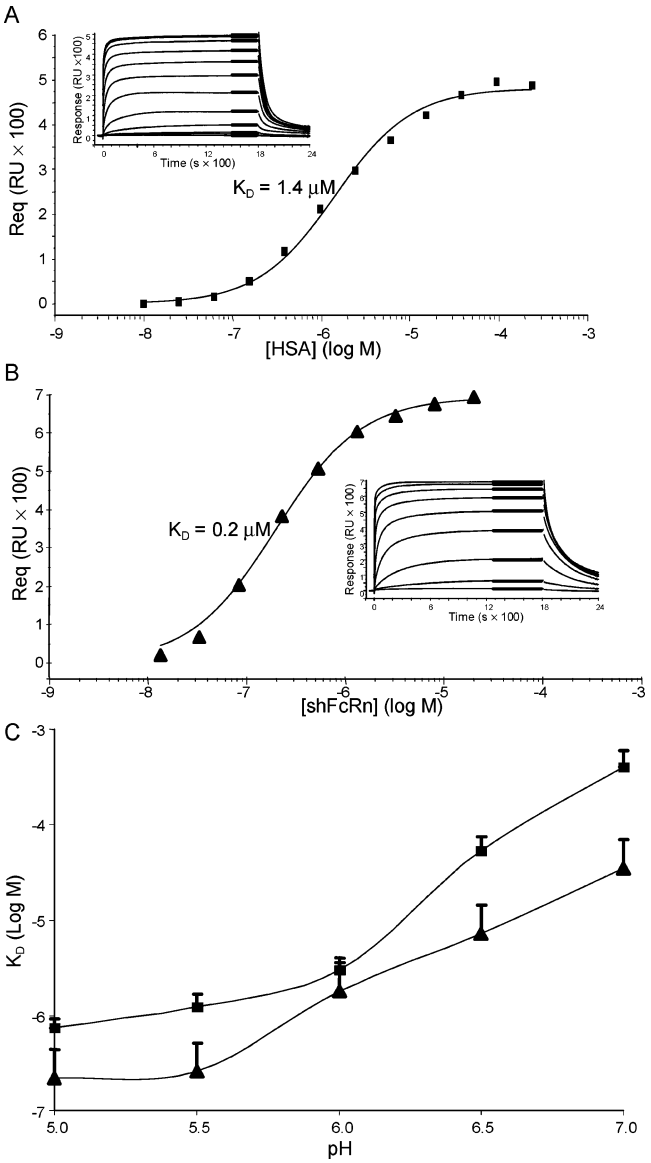

FIGURE 3: Surface plasmon resonance measurements show reversible binding of HSA and shFcRn with a pH-dependent increase in K_D. Increasing concentrations of HSA (10 nM−237 μM) or shFcRn (13 nM−20 μM) were injected at pH 5.5 for 1800 s over flow cells to which shFcRn (1128 RU) or HSA (1375 RU) had been immobilized. The RU at equilibrium (R_{eq}) for each injection were plotted (squares and triangles for immobilized shFcRn and HSA, respectively) vs the ligand concentrations, and the data were fit (solid curves) to a steady-state affinity model to calculate K_D for immobilized shFcRn (panel A) and HSA (panel B). The sensorgrams in the inset show the mass (resonance units) of analyte bound to immobilized ligand on the *Y*-axis after blank subtraction vs time in seconds on the *X*-axis. The relative residual for each data point was less than 4% of the predicted value. K_D was similarly measured over a pH 5−7 range at 0.5 pH increments after immobilizing shFcRn (squares) or HSA (triangles) (panel C). The plots show K_D on the *Y*-axis and pH on the *X*-axis. Values are the means ± standard deviations from six flow cells (coupling density ranging between 500 and 1500 RU) in two separate experiments.

(173-fold) (Figure 3C). However, the 583-fold difference observed for immobilized shFcRn is not very precise as shown by the large standard deviation (408 ± 195 μM), because high K_D values such as those observed at pH 7.0 cannot be accurately measured under the experimental conditions. Flow cells with ligand densities ranging between 500 and 1500 RU gave similar K_D values. The fit of the data to a single class of binding sites and K_D at pH 6.0 is similar to that obtained in ITC measurements (Figure 2B).

The pH-dependent increase in K_D suggests that FcRn may transport and protect albumin by the same mechanism as IgG but such a mechanism necessitates that the $t_{1/2}$ of the FcRn−albumin complex be compatible with the rapid kinetics required for binding at the acidic pH of the endosome and release at the neutral pH of the cell surface. To ascertain the $t_{1/2}$ of the shFcRn−HSA complex at acidic and neutral pH and to assess whether the increase in K_D with pH is governed by a decrease in k_a or an increase in k_d or both, we measured the k_a and k_d of the shFcRn−HSA interaction for both immobilized HSA and shFcRn (Figure 4). For both immobilized shFcRn (Figure 4A) and HSA (Figure 4C) the kinetic data fit the 1:1 binding model better than a model describing sequential binding of two sites on the analyte (bivalent analyte) or a model describing one analyte binding independently to two nonidentical sites on the ligand (heterogeneous ligand), unlike IgG and rat FcRn (*25*). These results agree with the single class of binding sites observed in our equilibrium binding SPR and ITC measurements. The k_a and k_d for the entire pH range of 5.0−7.0 were measured on the same immobilized shFcRn or HSA surface. The $t_{1/2}$ of the shFcRn−HSA complex at pH 5.0 and 7.0 for immobilized FcRn was 120 and 5 s at pH 5.0 and 7.0, respectively, while that for immobilized HSA was 110 s (pH 5.0) and 12 s (pH 7.0). For immobilized shFcRn, the k_a or k_d did not change appreciably between pH 5.0 and pH 6.0, but the k_a decreased sharply as the pH increased from 6 to 6.5 and showed a less pronounced decrease as the pH increased to 7.0. The k_d increased in 3-fold increments when the pH was increased from 6 to 6.5−7.0 (Figure 4B). For immobilized HSA, both k_a and k_d were practically unaltered between pH 5.0 and pH 5.5 but changed uniformly and reciprocally in 2−2.5-fold increments for every 0.5 pH unit increase (Figure 4D). As in the equilibrium experiments (Figure 3), flow cells with ligand densities ranging between 500 and 1500 RU gave similar k_a and k_d values. Thus, k_a and k_d both contribute to the increase in K_D with pH. Accurate kinetic measurements at high pH values were not possible because the dissociation rates were very rapid, and rapid association kinetics result from the high protein concentrations required to observe binding (*7*). The K_D values derived from the ratio of k_d and k_a measured in the kinetic experiments were in close agreement with those measured in equilibrium experiments for the entire pH range of 5.0−7.0. Thus, these two independent measurements corroborate each other (Table 1).

We wished to determine whether HSA binding to FcRn could be localized to one of the three independently folding domains of HSA: either domain I (D-I), domain II (D-II), or domain III (D-III). Each of these domains has been separately cloned and expressed in *Pichia pastoris* and has been shown to fold properly on the basis of near-UV−CD and far-UV−CD measurements and to bind ligand appropriately on the basis of induced CD measurements (*16*). We measured the capacity of the individual HSA domains to bind immobilized shFcRn by SPR (Figure 5A). D-I, D-II, and D-I-II (a single fragment encompassing both domains) showed no measurable binding to immobilized shFcRn, but D-III showed a binding response (97 RU) approximately one-third of that observed with HSA, our positive control (333

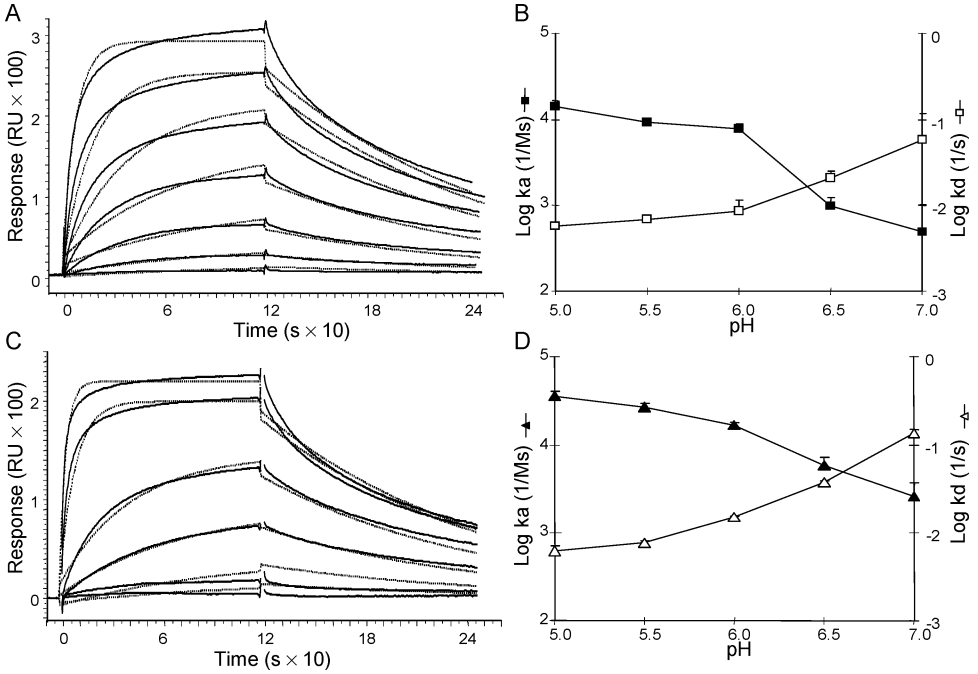

FIGURE 4: The increase in K_D with pH, measured by SPR, is governed by rapid association and dissociation kinetics and a reciprocal relationship between k_a and k_d. Increasing concentrations of HSA or shFcRn were injected at pH 5.5 over a flow cell to which shFcRn (606 RU) (panel A) or HSA (526 RU) (panel C) had been immobilized. The sensorgrams show the binding response (RU) of analyte to immobilized ligand after blank subtraction on the *Y*-axis and time in seconds on the *X*-axis (solid lines) and the fit of the data to the 1:1 binding model (dashed lines). The relative residuals for fitting the data were less than 3% of the predicted value. The k_a (solid symbols) and k_d (open symbols) for immobilized shFcRn (squares) and HSA (triangles), measured over a pH 5−7 range at 0.5 pH increments, are plotted on the *Y*-axis vs pH on the *X*-axis (panels B and D). Values are the means ± standard deviations from six flow cells (coupling density ranging between 500 and 1500 RU) in two separate experiments.

Table 1: SPR-Derived Kinetic and Equilibrium Constants for shFcRn and HSA Interaction at Various pHs[a]

	kinetic				
pH	$k_a \times 10^3$ [1/(M s)]	$k_d \times 10^{-3}$ [1/(M s)]	$t_{1/2}$ (s)	$k_d/k_a = K_D$ (μM)	equilibrium K_D (μM)
		Immobilized shFcRn			
5.0	14 ± 2.5	5.8 ± 0.3	119	0.4 ± 0.0	0.7 ± 0.2
5.5	9.3 ± 0.0	6.9 ± 0.6	100	0.7 ± 0.2	1.2 ± 0.4
6.0	7.7 ± 1.1	8.5 ± 3.0	81	1.1 ± 0.5	3.0 ± 1.0
6.5	1.0 ± 0.2	21.0 ± 3.7	33	21.6 ± 5.8	53.0 ± 23.0[b]
7.0	0.5 ± 0.5[b]	58.0 ± 61[b]	12	116.6 ± 63.6[b]	408.0 ± 195[b]
		Immobilized HSA			
5.0	35.9 ± 4.1	6.3 ± 0.7	110	0.2 ± 0.0	0.2 ± 0.0
5.5	27.0 ± 2.6	7.8 ± 0.4	89	0.3 ± 0.0	0.2 ± 0.0
6.0	16.6 ± 1.5	15.2 ± 0.4	46	0.9 ± 0.1	1.8 ± 0.1
6.5	5.9 ± 1.3	37.3 ± 1.7	19	6.5 ± 1.1	7.1 ± 1.2
7.0	2.6 ± 1.2[b]	138 ± 13.4[b]	5	72.8 ± 60.3[b]	34.7 ± 19.4[b]

[a] The equilibrium and kinetic constants were measured in experiments described in Figures 1 and 4, respectively. [b] These values are imprecise (and have large standard deviation) because K_D is very large at higher pH values, and for interactions with large K_D the kinetic data cannot be precisely modeled to calculate accurate rate constants. For the equilibrium binding data, impractically high concentrations of analyte are needed for accurate K_D measurement at pH 7.0.

RU), under saturating conditions. This one-third binding ratio of D-III to HSA suggests equimolar binding since the molecular mass of D-III (23.3 kDa) is approximately one-third of HSA (66.7 kDa). This experiment was performed twice with similar results. The small measurable response (7 RU) observed with D-I-II in this experiment was not replicable and was therefore ignored. We also tested the ability of all the possible combinations of these domains to bind shFcRn and found that injecting other domains in combination with D-III had no effect on D-III−shFcRn binding, suggesting that the domains neither cooperate in shFcRn binding nor associate with each other in solution. To ensure that the domains were still intact, all were analyzed by SDS−PAGE (Figure 5B). Densitometry of the Commassie-stained gel showed that at least 90% of the signal in each lane corresponded to the molecular mass of the bona fide domain; proteolytic degradation is thus an unlikely explanation for the failure of D-I, D-II, and D-I-II to bind shFcRn.

DISCUSSION

We conclude from these data that FcRn binds both albumin and IgG at distinct, nonoverlapping sites and IgG neither competes nor cooperatively influences FcRn−albumin binding. Unlike the FcRn−IgG interaction, the FcRn−albumin binding is hydrophobic in nature with one albumin molecule binding one molecule of FcRn. The interaction is characterized by a single class of binding sites with an affinity in the low micromolar range at acidic pH, unlike the two classes of binding sites with different affinities (nanomolar and submicromolar) reported for the FcRn−IgG interaction. FcRn's affinity for albumin decreases with increasing pH, and the interaction has rapid dissociation kinetics, suggesting that, despite the disparities in the mechanism of interaction of FcRn and albumin relative to IgG, the overall mechanism of albumin protection from a degradative fate is similar to that of IgG.

The FcRn−albumin binding is characterized by an unfavorable enthalpy change (ΔH) but a large favorable entropy change (ΔS), a feature characteristic of hydrophobic interactions (*22*, *26*, *27*). This unique feature of the FcRn−albumin interaction distinguishes it from the FcRn−IgG interaction,

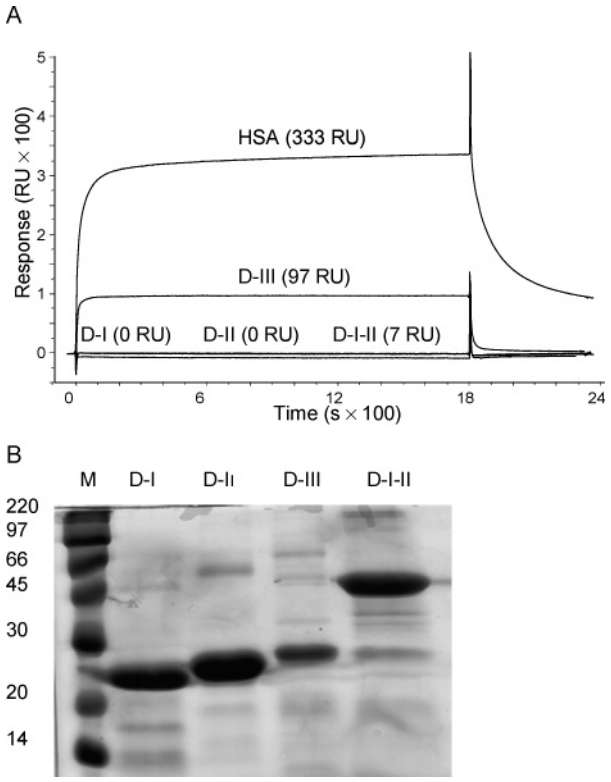

FIGURE 5: SPR shows that only domain III of HSA binds shFcRn. Panel A: Various recombinant domains of HSA and native HSA at 10 μM were injected at 5 μL/min over immobilized shFcRn (725 RU) for 1800 s at pH 5.5. The binding response at equilibrium was measured and is indicated by the numbers in parentheses. Various combinations of these domains, D-I-II + D-III, D-II + D-III, D-I + D-III, and D-I + D-II + D-III, when injected over the same immobilized shFcRn surface showed binding responses comparable to that obtained with D-III alone (data not shown). Panel B shows a Commassie-stained 15% SDS−PAGE of all of the HSA domain preparations that were used in the SPR experiment. M indicates molecular mass markers in kDa; D followed by Roman numerals indicates purified preparations of recombinant domains and a single recombinant fragment including domains I and II (5 μg of protein per lane).

which has been shown to be driven by a favorable ΔH and a relatively small favorable ΔS (*20*). Moreover, binding of several fatty acids, liposomes, surfactants, and drugs to albumin has been shown to be exothermic and largely enthalpy driven with the exception of some site I binding of heterocyclic drugs that are entropically driven with a minor favorable ΔH (*28*−*32*).

Kinetic and equilibrium measurements show that like the FcRn−IgG complex the affinity of the FcRn−albumin complex is exquisitely sensitive to pH, being reduced by over 2 orders of magnitude as the pH is raised from 5.0 to 7.0. Moreover, like the FcRn−IgG complex ($t_{1/2}$ decreases 10−30-fold; 420−558 s at pH 6.0 and 18−60 s at pH 7.0) the $t_{1/2}$ of the FcRn−albumin complex decreases 10−20-fold when the pH is increased from acidic (110−120 s at pH 5.0) to neutral (5−12 s at pH 7.0) (*7*). These data support the proposed role of FcRn as a protection receptor for albumin whereby FcRn binds albumin with high affinity in the acidic endosome, diverts it away from the lysosomal degradation pathway, and releases it at the slightly basic pH of the cell surface where the affinity of FcRn for albumin is decreased and the dissociation rate is rapid. Both FcRn and albumin are then free to recycle. The functional effect of this protective salvage cycle is to prolong the life span of albumin. The role of FcRn in albumin salvage is also indicated by the observation that FcRn KO mice have shorter albumin half-lives (*13*).

Comparing the kinetics of the FcRn−albumin interaction with that of peptide binding to MHC I and MHC II molecules, we find that, unlike the much slower kinetics of peptide binding to MHC I and II molecules ($t_{1/2}$ of 83 and 45 min, respectively), FcRn−albumin association and dissociation kinetics are very rapid, suggesting that the FcRn−albumin interaction is mechanistically different from the MHC−peptide binding but similar to the FcRn−IgG interaction (*7*, *33*−*35*). The kinetic rate constants show that the increase in K_D with pH is due to reciprocal changes in k_a and k_d. Such pH-dependent binding has also been reported for peptide binding by MHC II molecules, but pH dependence is governed by a decrease in association rate while the dissociation rate remains unchanged (*36*).

The pH dependence of the FcRn−albumin interaction suggests that, like IgG, albumin binding to the receptor might also be mediated through titratable histidine residues. An alignment of the amino acid sequences of the α-chains of FcRn from nine species of mammals [human, rat, mouse, bovine, possum, macaque, dromedar, pig, and sheep (Dr. Imre Kacskovics, Szent István University, Budapest, Hungary, personal communication)] reveals a likely candidate histidine on the receptor. Of the eight histidines in human FcRn (hFcRn) only H166 is conserved in all nine FcRn sequences, but it is expressed in only a small fraction (6 of 87) of randomly chosen MHC I sequences. H166 (H168 in rat) is not involved in IgG or b2m interaction according to mutational and crystallographic studies of the rat FcRn (*4*, *6*). Another histidine, H263, in FcRn α-chain sequences is also conserved but is a nearly constant feature of all Ig domains (*4*). We speculate that albumin may bind at or near H166 on human FcRn.

The experiments measuring binding of FcRn to the three recombinant albumin domains establish that albumin D-III alone is both necessary and sufficient for binding to FcRn. Not only is D-III the only domain of the three to bind immobilized shFcRn, but D-III binding is equimolar to HSA binding. Amino acid sequence alignment of D-III of albumin from different species (rat, bovine, mouse, and human) that have been shown to bind shFcRn (unpublished data) reveals that, of the four histidines in D-III (H440, H464, H510, H535), three are conserved (H464, H510, H535). It has been shown that H464 undergoes pH-dependent protonation between pH 5.0 and pH 7.0 during the N−B transition of albumin, suggesting a potential for histidine-mediated pH-dependent interaction with FcRn (*37*).

Conserved histidine residues are, therefore, positioned on both the receptor and the ligand to account for histidine-mediated pH-dependent binding. Determining whether the histidines on the receptor, ligand, or both are involved in binding and, more importantly, if histidine residues are at all involved in the FcRn−albumin interaction will require mutational analysis beyond the scope of our present study. The possibility that pH-dependent binding occurs due to a conformational change in the receptor as has recently been reported for FcRY cannot be ruled out (*38*). This explanation is, however, less likely considering that FcRn does not undergo any pH-dependent conformational changes (*4*, *6*, *7*, *38*, *39*).

ACKNOWLEDGMENT

We thank Dr. P. J. Bjorkman for the shFcRn-producing cells and for helpful discussions. We acknowledge Dr. Craig McElroy for assistance with ITC.

SUPPORTING INFORMATION AVAILABLE

Effect of HSA aggregates on SPR measurements, dynamic light scattering analysis, and size exclusion chromatography and one figure showing that monomeric albumin binding to immobilized FcRn is similar to unresolved albumin. This material is available free of charge via the Internet at http://pubs.acs.org.

REFERENCES

1. Brambell, F. W. R. (1970) *The Transmission of Passive Immunity from Mother to Young*, North-Holland Publishing Co., Amsterdam.
2. Kim, J. K., Tsen, M. F., Ghetie, V., and Ward, E. S. (1994) Localization of the site of the murine IgG1 molecule that is involved in binding to the murine intestinal Fc receptor, *Eur. J. Immunol. 24*, 2429−2434.
3. Burmeister, W. P., Huber, A. H., and Bjorkman, P. J. (1994) Crystal structure of the complex of rat neonatal Fc receptor with Fc, *Nature 372*, 379−383.
4. Raghavan, M., Chen, M. Y., Gastinel, L. N., and Bjorkman, P. J. (1994) Investigation of the interaction between the class I MHC-related Fc receptor and its immunoglobulin G ligand, *Immunity 1*, 303−315.
5. Medesan, C., Matesoi, D., Radu, C., Ghetie, V., and Ward, E. S. (1997) Delineation of the amino acid residues involved in transcytosis and catabolism of mouse IgG1, *J. Immunol. 158*, 2211−2217.
6. Martin, W. L., West, A. P., Gan, L., and Bjorkman, P. J. (2001) Crystal structure at 2.8 Å of an FcRn/heterodimeric Fc complex: Mechanism of pH-dependent binding, *Mol. Cell 7*, 867−877.
7. Raghavan, M., Bonagura, V. R., Morrison, S. L., and Bjorkman, P. J. (1995) Analysis of the pH dependence of the neonatal Fc receptor/immunoglobulin G interaction using antibody and receptor variants, *Biochemistry 34*, 14649−14657.
8. Simister, N. E., and Mostov, K. E. (1989) An Fc receptor structurally related to MHC class I antigens, *Nature 337*, 184−187.
9. Junghans, R. P. (1997) The Brambell receptor (FcRB): mediator of transmission of immunity and protection from catabolism for IgG, *Immunol. Res. 16*, 29−57.
10. Ghetie, V., and Ward, E. S. (2000) Multiple roles for the major histocompatibility complex class I-related receptor FcRn, *Annu. Rev. Immunol. 18*, 739−766.
11. Waldmann, T. A., and Strober, W. (1969) Metabolism of immunoglobulins, *Prog. Allergy 13*, 1−110.
12. Schultze, H. E., and Heremans, J. F. (1966) *Molecular Biology of Human Proteins: With Special Reference to Plasma Proteins. Vol. 1. Nature and Metabolism of Extracellular Proteins*, Elsevier, New York.
13. Chaudhury, C., Mehnaz, S., Robinson, J. M., Hayton, W. L., Pearl, D. K., Roopenian, D. C., and Anderson, C. L. (2003) The major histocompatibility complex-related Fc receptor for IgG (FcRn) binds albumin and prolongs its lifespan, *J. Exp. Med. 197*, 315−322.
14. Kim, J., Bronson, C. L., Hayton, W. L., Radmacher, M. D., Roopenian, D. C., Robinson, J. M., and Anderson, C. L. (2005) Albumin turnover: FcRn-mediated recycling saves as much albumin from degradation as the liver produces, *Am. J. Physiol. Gastrointest. Liver Physiol.* (doi:10.1152/ajpgi.00286.2005).
15. West, A. P., Jr., and Bjorkman, P. J. (2000) Crystal structure and immunoglobulin G binding properties of the human major histocompatibility complex-related Fc receptor, *Biochemistry 39*, 9698−9708.
16. Dockal, M., Carter, D. C., and Rüker, F. (1999) The three recombinant domains of human serum albumin: Sturctural characterization and ligand binding properties, *J. Biol. Chem. 274*, 29303−29310.
17. Gill, S. C., and Hippel, P. H. (1990) Calculation of protein extinction coefficients from amino acid sequence data, *Anal. Biochem. 182*, 319−326.
18. Leach, J. L., Sedmak, D. D., Osborne, J. M., Rahill, B., Lairmore, M. D., and Anderson, C. L. (1996) Isolation from human placenta of the IgG transporter, FcRn, and localization to the syncytiotrophoblast: Implications for maternal-fetal antibody transport, *J. Immunol. 157*, 3317−3322.
19. Limbird, L. E. (1986) *Cell Surface Receptors*: *A Short Course on Theory and Methods*, Martinus Nijhoff, Boston.
20. Huber, A. H., Kelley, R. F., Gastinel, L. N., and Bjorkman, P. J. (1993) Crystallization and stoichiometry of binding of a complex between a rat intestinal Fc receptor and Fc, *J. Mol. Biol. 230*, 1077−1083.
21. Pierce, M. M., Raman, C. S., and Nall, B. T. (1999) Isothermal titration calorimetry of protein−protein interactions, *Methods 19*, 213−221.
22. Leavitt, S., and Freire, E. (2001) Direct measurement of protein binding energetics by isothermal titration calorimetry, *Curr. Opin. Struct. Biol. 11*, 560−566.
23. Vaughn, D. E., and Bjorkman, P. J. (1997) High-affinity binding of the neonatal Fc receptor to its IgG ligand requires receptor immobilization, *Biochemistry 36*, 9374−9380.
24. Peters, T., Jr. (1996) *All about Albumin*: *Biochemistry, Genetics, and Medical Applications*, Academic Press, New York.
25. Martin, W. L., and Bjorkman, P. J. (1999) Characterization of the 2:1 complex between the class I MHC-related Fc receptor and its Fc ligand in solution, *Biochemistry 38*, 12639−12647.
26. Jelesarov, I., and Bosshard, H. R. (1998) Isothermal titration calorimetry and differential scanning calorimetry as complementary tools to investigate the energetics of biomolecular recognition, *J. Mol. Recognit. 12*, 3−18.
27. Velazquez-Campoy, A., Todd, M. J., and Freire, E. (2000) HIV-1 protease inhibitors: enthalpic versus entropic optimization of the binding affinity, *Biochemistry 39*, 2201−2207.
28. Aki, H., and Yamamoto, M. (1994) Thermodynamic characterization of drug binding to human serum albumin by isothermal titration microcalorimetry, *J. Pharm. Sci. 83*, 1712−1716.
29. Liu, R., Meng, Q., Xi, J., Yang, J., Ha, C., Bhagavan, N. V., and Eckenhoff, R. G. (2004) Comparative binding character of two general anaesthetics for sites on human serum albumin, *Biochem. J. 380*, 147−152.
30. Aki, H., and Yamamoto, M. (1989) Thermodynamics of the binding of phenothiazines to human plasma, human serum albumin and alpha 1-acid glycoprotein: a calorimetric study, *J. Pharm. Sci. 41*, 674−679.
31. Nielsen, A. D., Borch, K., and Westh, P. (2000) Thermochemistry of the specific binding of C12 surfactants to bovine serum albumin, *Biochim. Biophys. Acta 1479*, 321−331.
32. Dimitrova, M. N., Matsumura, H., Dimitrova, A., and Neitchev, V. Z. (2000) Interaction of albumins from different species with phospholipid liposomes. Multiple binding sites system, *Int. J. Biol. Macromol. 27*, 187−194.
33. Christinck, E. R., Luscher, M. A., Barber, B. H., and Williams, D. B. (1991) Peptide binding to class I MHC on living cells and quantitation of complexes required for CTL lysis, *Nature 352*, 67−70.
34. Ceppellini, R., Frumento, G., Ferrara, G. B., Tosi, R., Chersi, A., and Pernis, B. (1989) Binding of labelled influenza matrix peptide to HLA DR in living B lymphoid cells, *Nature 339*, 392−394.
35. Boyd, L. F., Kozlowski, S., and Margulies, D. H. (1992) Solution binding of an antigenic peptide to a major histocompatibility complex class I molecule and the role of b2-microglobulin, *Proc. Natl. Acad. Sci. U.S.A. 89*, 2242−2246.
36. Reay, P. A., Wettstein, D. A., and Davis, M. M. (1992) pH dependence and exchange of high and low responder peptides binding to a class II MHC molecule, *EMBO J. 11*, 2829−2839.
37. Bos, O. J. M., Labro, J. F. A., Fischer, M. J. E., Wilting, J., and Janssen, L. H. M. (1989) The molecular mechanism of the neutral-to-base transition of human serum albumin, *J. Biol. Chem. 264*, 953−959.
38. West, A. P., Herr, A. B., and Bjorkman, P. J. (2004) The chicken yolk sac IgY receptor, a functional equivalent of the mammalian MHC-related Fc receptor, is a phospholipase $A_{2\ \text{receptor homolog}}$, *Immunity 20*, 601−610.
39. Vaughn, D. E., and Bjorkman, P. J. (1998) Structural basis of pH-dependent antibody binding by the neonatal Fc receptor, *Structure 6*, 63−73.

BI052628Y